Turbid Media Extinction Coefficient for Near-Infrared Laser Radiation

T Dreischuh, L Gurdev, O Vankov, D Stoyanov, L Avramov

Institute of Electronics, Bulgarian Academy of Sciences
72 Tzarigradsko chaussee Blvd., 1784 Sofia, Bulgaria

E-mail: tanjad@ie.bas.bg, lugurdev@ie.bas.bg

Abstract. In this work, extended investigations are performed of the extinction coefficient of Intralipid-20% dilutions in distilled water depending on the Intralipid concentration, for laser radiation wavelengths in the red and near-infrared regions covering the so-called tissue optical window. The extinction is measured by using an approach we have developed recently based on the features of the spatial intensity distribution of laser-radiation beams propagating through semi-infinite turbid media. The measurements are conducted using separately two dilution-containing plexiglass boxes of different sizes and volumes, in order to prove the appropriateness of the assumption of semi-infinite turbid medium. The experimental results for the extinction are in agreement with our previous results and with empiric formulae found by other authors concerning the wavelength dependence of the scattering coefficient of Intralipid - 10% and Intralipid - 20%. They are also in agreement with known data of the water absorptance. It is estimated as well that the wavelengths around 1320 nm would be advantageous for deep harmless sensing and diagnostics of tissues.

1. Introduction

The investigations in the fields of optical diagnostics and therapy [1-3] are based on the knowledge of the optical characteristics (parameters) of tissue and tissue-like phantoms. The main such characteristics from biomedical point of view are: the absorption coefficient μ_a describing the optical - energy dissipation and the thermal effect on tissues; the integral scattering, μ_s, backscattering, μ_{bs}, and reduced-scattering, $\mu_{rs} = \mu_s(1-g)$, coefficients describing the optical-energy dispersion; the extinction (total attenuation) coefficient $\mu_e = \mu_a+\mu_s$; and the scattering anisotropy factor, g. The backscattering and extinction coefficients determine the informative depth of light penetration in tissue, from where the (single-sided tomography) signal is strong enough to be accurately detected.

The use of phantoms is necessary to avoid tedious and complicated in vivo experimental procedures for testing and calibration of novel diagnostic and therapeutic methods and instruments. The dilutions of Intralipid (IL) fat emulsions in distilled water [4-8] are an important class of liquid phantoms having numerous advantages. Certainly, the optical properties of tissues and phantoms determine the radiative transfer inside such media. Moreover, they condition the therapeutic effects in tissues as well as the possibility of specifying characteristic inhomogeneities in tissue diagnostics. Therefore, the determination of the optical characteristics and the development of methods for this purpose are of primary importance for the biomedical photonics of tissues [9,10]. The optical radiation wavelengths λ employed in the biomedical photonics cover the interval from 600 nm to 1300 nm, where the absorption in tissues (mainly in water) is minimal: from 0.002 cm^{-1} at λ = 600 nm to ~1.35

cm^{-1} at λ = 1300 nm [11-13]. This wavelength interval is often called the tissue optical (or therapeutic) window [14]. The scattering coefficient of tissues for radiation from the optical window is orders of magnitude larger than the corresponding absorption coefficient. Thus, the tissues are turbid media for such radiation.

The main goals of the present work are as follows. First, using an approach we have developed recently [15,16], to determine experimentally the extinction coefficient of Intralipid dilutions in distilled water, for laser radiation of different wavelengths within the tissue therapeutic window. Another aim is to perform a comparison and mutual validation of the results for μ_e obtained here and corresponding results for μ_s obtained using empiric formulae derived by other authors [6-8]. The third goal is to prove experimentally the assumption that the plexiglass boxes employed containing the IL dilutions are sufficiently large to be considered as semi-infinite turbid media. At last, the work is also intended to estimate and illustrate the eventual advantage of using long-wavelength laser radiation (around the upper limit of the therapeutic window) for deeper harmless diagnostics of tissues.

The theoretical basis of the method of measuring the extinction, the experimental arrangements and procedures, and the materials employed are described in the following section 2. In section 3, the experimental results are analysed and discussed and compared with results obtained by other authors. In section 4, possible diagnostic advantages of longer-wavelength laser radiation are evaluated and discussed. The main results of the work are summarized in section 5.

2. Methods, experimental procedures and phantoms

2.1. Extinction measurement approach

The extinction (total attenuation) coefficient of the Intralipid dilutions of interest, occupying large plexiglass containers, has been determined by measuring the longitudinal, in-depth profile of the on-axis intensity ($\propto$ the detected small-receiving-aperture gated light power) of forward propagating inside laser radiation beams. The depth in the IL dilutions is given by the coordinate z along the beam axis $0z$ that is perpendicular to and begins from the internal frontal wall of the container (figure 1). Like tissues, the IL dilutions produce forward-peaked scattering of light, mainly within a $\sim\gamma_m = [2(1-g)]^{1/2}$ – wide angular interval. Then, the spatial (transversal and in-depth) distribution of the forward-propagating light intensity is analytically obtainable as a small-angle solution of the radiative-transfer equation [16,17]. This solution is valid to depths several times as large as the transport mean free path of the photon μ_{rs}^{-1} in the investigated medium. Simple analytical expressions of the on-axis detected power $J(z)$ are obtained [16] for the low-scattering zone, where $\mu_s z \sim 1$ or $\mu_s z < 1$ and the single-scattered and unscattered light is prevailing, and the developed-scattering zone, where $\mu_s z >> 1$ and the multiple-scattering light is prevailing. The expression of $J(z)$ in the low-scattering zone have different forms, depending on the relation between γ_m and the angle of acceptance γ of the receiving optical system. When $\gamma >> \gamma_m$, $J(z)$ drops down exponentially with z, with decay constant μ_a, when $z < (w^2 + E^2)^{1/2}$, and with decay constant μ_e, when $z > (w^2 + E^2)^{1/2}$; w and E are the radii of the sensing (collimated) laser beam at z=0 and of the receiving aperture, respectively. When $\gamma << \gamma_m$, $J(z)$ decreases exponentially with only one decay constant μ_e. In the developed-scattering zone, $J(z)$ behaves $\propto z^{-3}\exp(-\mu_a z)$ or $z^{-4}\exp(-\mu_a z)$ when $\gamma^2 >> \mu_{rs} z$ or $\gamma^2 << \mu_{rs} z$, respectively. In the experiments performed, the conditions $\gamma << \gamma_m$ and $\gamma^2 << \mu_{rs} z$ are in power. Under these conditions, $J(z) \propto z^{-4}\exp(-\mu_a z)$, in the developed-scattering zone, and

$$J(z) = J_0 \exp(-\mu_e z)[1 + \delta(z, \mu_s, w, \gamma, E, g)] \quad (1)$$

in the low-scattering zone, where $J_0 = P_t(E^2/w^2)$, P_t is the incident beam power, and δ is a term that is negligible to some depth z_n decreasing with the increase of the turbidity ($\propto \mu_s$) of the medium under

investigation. According to (1), a log-linear fit of the experimental data obtained for $J(z)$ in the low-scattering zone, at $\gamma << \gamma_m$ and $\delta << 1$, allows one to determine the extinction coefficient.

2.2. Experimental

The experimental setup for measuring the forward-propagating light power $J(z)$ is schematically shown in figure 1. The light sources employed are laser diodes emitting nearly collimated continuous-wave optical beams of about 1 mm radius and wavelengths λ = 672 nm, 847 nm, and 1326 nm. The Intralipid dilutions under investigation have been placed in two plexiglass boxes having parallelepiped and cubic forms with sizes of 12×12×22 cm and 25 cm side, respectively. The axis of the incident laser beam is perpendicular to the entrance wall of the container and is considered as coincident with the axis $0z$ beginning from the internal entry wall of the container and oriented forward, in the direction of incidence of the beam (figure 1). The forward-propagating light power inside the container is measured by using a scanning optical fiber of $2E$ = 0.1 mm core diameter and $\gamma \sim 9°$ (~ 0.16 rad) half angle of acceptance. The fiber is oriented antiparallel to the beam axis and is connected with an optical radiometer Rk-5100 (Laser precision corp., USA) in external locking regime, with a RqP-546 silicon probe for 672 and 847 nm radiation, and a RkP-545 pyroelectric probe for 1326 nm radiation, a 14bits ADC and a computer for appropriate data processing. The noise equivalent power (NEP) of the radiometer is 2.10^{-12} W, with RqP-546, and 2.10^{-7} W, with RkP-545. Its averaging (low-pass filtering) time constant τ_a is chosen to be 1 s. The on-axis detected-power distribution (on-axis intensity profile) is measured by a longitudinal scan of the fiber along the beam axis, implemented by using a linear translation stage with an integrated stepper motor and controller LTS 300/M (Thorlabs, Inc., USA). In the experiments, the sampling step is varied from 0.1 mm to 10 μm. They have been performed in a dark environment at practically entirely damped stray light influence. The least measured power values of interest exceed considerably the NEP of the radiometer. Thus, the data fluctuations should result from the signal-conditioned shot noise, digitizing noise, laser power fluctuations, and scintillations due to the random walk of the scattering particles. By the low-pass filtering performed with time constant 1 s, along with 400 measurements per point, the fluctuation level is reduced to about 1% for all the wavelengths at the least sampling steps employed.

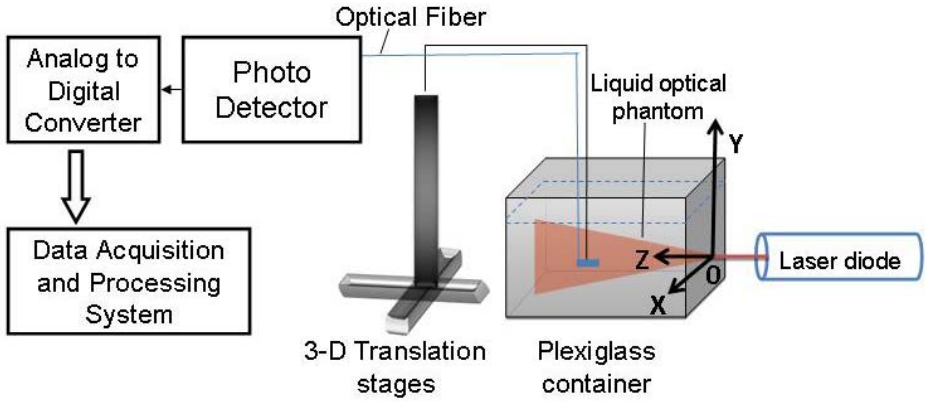

Figure 1. Experimental setup.

2.3. Intralipid phantoms

The turbid media investigated in the work are dilutions in distilled water of different amounts (volume parts) of Intralipid-20% (Fresenius Kabi AB, Sweden). The IL concentration has usually been defined as the volume fraction of soybean oil and egg lecithin forming the scattering submicron pellets in the dilution [6]. The volume fraction of these components is 22.74% in stock IL-20% and 11.95%, in stock IL-10%. The dilutions (phantoms) are prepared just before the measurements performed at room temperature. The IL concentration varies from 0.02 to 3.2 % in volume for different wavelengths. The

Intralipid bags employed in the experiments described below are from the same production batch (#10GH5382).

3. Results and discussion

The measured on-axis light power profiles $J(z)$ involve both the low scattering and developed scattering zones. An illustration of such recorded profiles at different IL concentrations is given in figure 2. The exponential fall-off regions in the low-scattering zone are well distinguishable. As expected, the extent of these regions decreases with the increase of the IL concentration [15]. The measurements of the profiles $J(z)$ have been performed repeatedly by using both the above-described plexiglass containers, the larger cubic box and the smaller one having parallelepiped form.

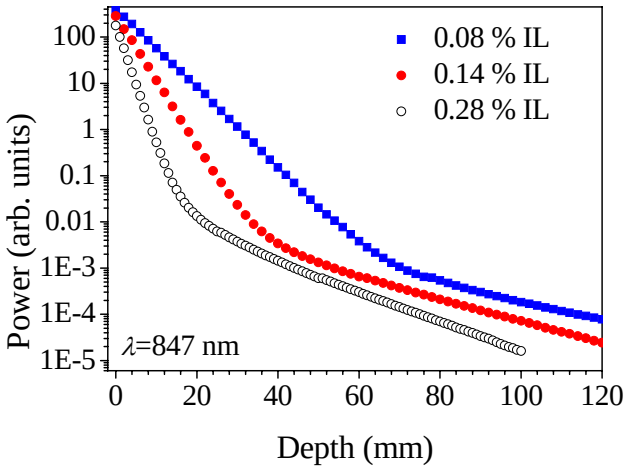

Figure 2. Measured in-depth light power profiles $J(z)$ for different Intralipid concentrations.

The log-linear fit of the results obtained for $J(z)$ in the low-scattering zone provides the values of the extinction coefficient μ_e for the wavelengths of interest. The dependence of the results for μ_e on the IL concentration C is illustrated in figure 3 for $\lambda = 847$ nm and $\lambda = 1326$ nm. The values of μ_e obtained using both the containers are close to each other within the statistical accuracy. This allows one to assume that the investigated dilutions occupy large-enough volumes to be considered as semi-infinite turbid media. The dependence $\mu_e(C)$ indicates a linear run in general at relatively low IL concentrations, which is in agreement with the results obtained previously by us and other researchers [15,16,18,19]. At $\lambda = 1326$ nm a linear dependence is observed up to the maximum IL concentrations concerned in the experiments with the small box. The experimental points obtained in this case can also be well fitted by a quadratic function but with negligibly small nonlinearity. The analogous experiments conducted with the large box lead to analogous results covering the same fitting dependences up to 2% IL concentration (figure 3b). The further increase of the concentration, and respectively of the amount of liquid in the container, leads to already noticeable deformations of it and respectively to noticeable distortions (apparent nonlinearity) of the results for $\mu_e(C)$. At $\lambda = 847$ nm, the experimental points obtained with both the containers follow the same nonlinear-in-general dependence $\mu_e(C)$ up to 2% IL concentration again (figure 3a). Above this concentration, the experimental points obtained with the large box deviate down due to the above-mentioned reason. In this case, the (quadratic, found by fitting) nonlinearity is noticeable for IL concentrations above 0.3-0.5%. (The experimental points obtained for $C \leq 0.5$ % obey a linear good-fit dependence $\mu_e(C)$.) Such a nonlinear behaviour has also been observed previously [18] in experiments with low-concentration dilutions of milk. It is perhaps a stage of a more general nonlinear dependence of μ_s on C at higher IL-20% concentrations (up to 25%) observed in [20] and analyzed theoretically in [21]. The nonlinear run

of the extinction coefficient needs a profound and adequate physical explanation and mathematical description.

The experimental results show as well that with the increase of λ, the extinction coefficient μ_e decreases due to decreasing the light scattering (figure 4), and the interval of linearity at low IL concentrations extends.

The intercepts (μ_e at zero IL concentration) of the fitting curves in figure 4 are close to the published data for the absorption coefficients of pure water μ_{aw} (e.g., [11-13]). For instance, at λ = 1326 nm, the curve fitting all the experimental points has intercept $\mu_e(0) \sim 2.07$ cm^{-1} that practically coincides with the literature data. Thus, the method of measuring $\mu_e(C)$ and the results obtained can be assumed as reliable.

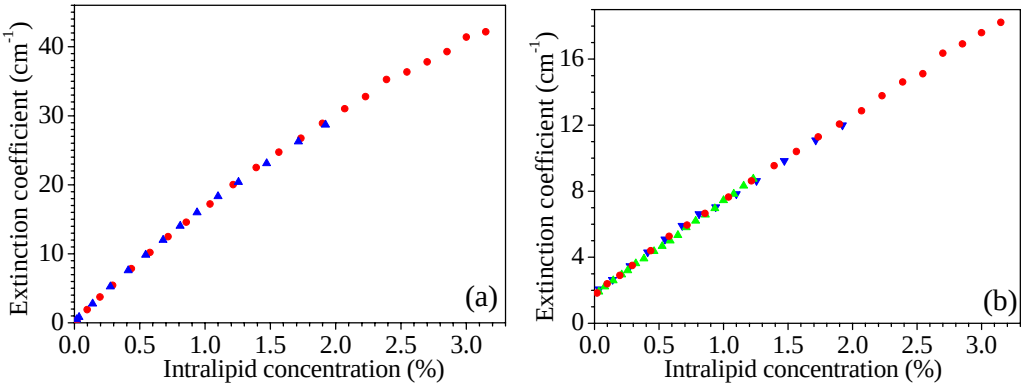

Figure 3. Extinction coefficients of Intralipid-20% dilutions, depending on the IL concentration, determined by using 12×12×22 cm box (circles) and 25×25×25 cm box (triangles) at λ = 847 nm (a) and λ = 1326 nm (b).

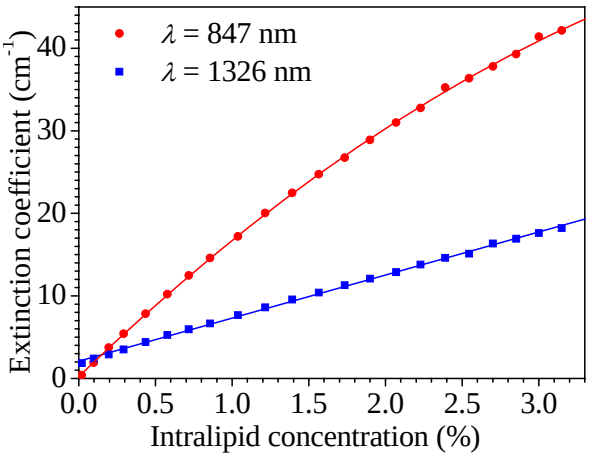

Figure 4. Extinction coefficients of dilutions with different Intralipid concentrations determined by using 12×12×22 cm box, at λ=847 nm (dots) and λ=1326 nm (squares), and the corresponding fitting curves.

There are derived in the literature [6-8] some empiric analytical expressions of the scattering coefficient μ_s of dilutions of IL-10% and IL-20%, as a function of λ. Such expressions have been derived from experimental data and Mie-theory calculations and help the estimation of the values of

μ_s, at different radiation wavelengths λ, depending on the IL concentration C. All the known empiric dependences $\mu_s(\lambda)$ can be written in a common form:

$$\mu_s(\lambda) = a\lambda^b \tag{2}$$

where λ is given in [μm], and μ_s in [$mL^{-1}Lcm^{-1}$], implying that the volume fraction of IL-10% or IL-20% (having 11.952% and 22.74% volume concentration of scattering particles, respectively) in distilled water is in units of [ml/l]. A first such expression concerning dilutions of IL-10% and the wavelength interval 0.4 μm ≤ λ ≤ 1.1μm, with a = 0.16 and b = -2.4, have been established by van Staveren et al. [6]. Two more similar expressions concerning dilutions of IL-20%, with $\lambda \in$ (0.4 μm, 1 μm), a = 0.249 and b = -2.397, and $\lambda \in$ (0.5 μm, 2.25 μm), a = 0.317 and b = -2.59, are given by Michels et al [7] and Aernouts et al [8].

In figure 5, the experimentally obtained results for $\mu_e(C)$ corrected for the absorption of water are compared with linearly extrapolated data $\mu_s(C)$ obtained on the basis of the above-discussed expressions (2). It is seen that at lower concentrations (say, C < 0.5 %), where the scattering is assumed independent and the extinction coefficient should depend linearly on the concentration, the experimental results for $\mu_e(C)$ and the extrapolated results for $\mu_s(C)$ nearly coincide. At larger concentrations, two pairs of near results are outlined. The first pair includes the extrapolated results, following from the formulae derived in [6] and [8]. The second pair includes the experimental results obtained here and those following from the formula of Michels et al. [7]. Such a proximity, especially of the experimental and extrapolated results, is a confirmation of the reliability, for different intervals of concentrations, of both the method for measuring μ_e and the empiric formulae.

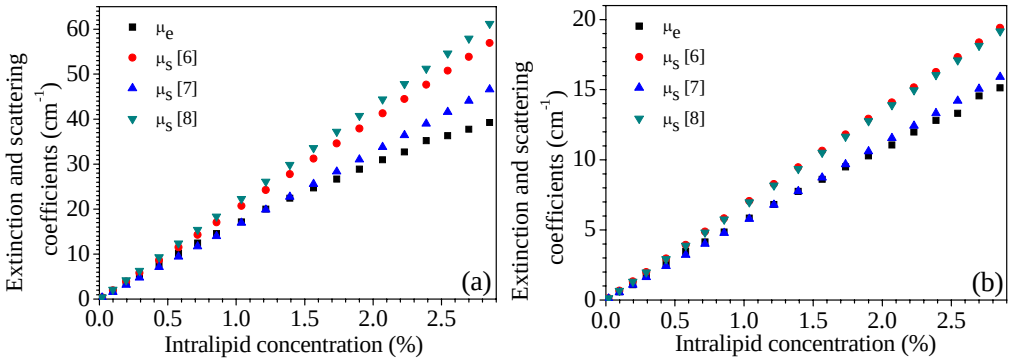

Figure 5. Experimentally-determined extinction coefficient μ_e (corrected for the absorption of water), as a function of the Intralipid concentration, compared with the scattering coefficient μ_s evaluated using the empiric formulae derived in [6-8] at λ = 847 nm (a) and 1326 nm (b).

4. Single-sided lidar-type sensing of turbid media

The smaller extinction and higher backscattering in tissue-like turbid media of laser radiation with longer wavelength λ would allow one to use such radiation for deeper sensing and diagnostics of tissues and other similar turbid media. A simple approximate illustration of such a possibility is given in figure 6, where, based on the single-scattering lidar equation [22], the normalized time-to-range resolved detected return power from a turbid medium, irradiated by laser pulses of wavelength λ = 672 nm, 847 nm, or 1326 nm, is evaluated as a function of the depth of sensing z. It is seen in the figure that the longer the wavelength the stronger the return signals from all the depths in the medium. The medium is chosen to be a 0.2% IL dilution with μ_e determined here (see also figure 4), and $\mu_s \sim \mu_e$ and g evaluated using the corresponding formulae of van Staveren et al. [6]. At an IL concentration of 0.2%, the low-scattering zone, where the lidar equation should still be valid, may achieve depths of the

order of centimeters (see also in [23]). For more clarity, let us write explicitly the lidar equation in the form [22]

$$S(z,\lambda) = \mu_{bs}(\lambda) \exp[-2\mu_e(\lambda)z] , \quad (3)$$

where $S(z,\lambda) = P_b(z,\lambda)/(E_p cA/2z^2)$ is the so-called lidar S function, $P_b(z,\lambda)$ is the detected, time-to-range resolved return power, c is the speed of light, E_p is the sensing pulse energy, and $A=\pi E^2$ is the receiving aperture area. For Henyey-Greenstein indicatrix, the backscattering coefficient

$$\mu_{bs} = [(1-g)/4\pi](1+g)^{-2}\mu_s , \quad (4)$$

and

$$g(\lambda) = 1.1-0.58\lambda \ [\mu m]. \quad (5)$$

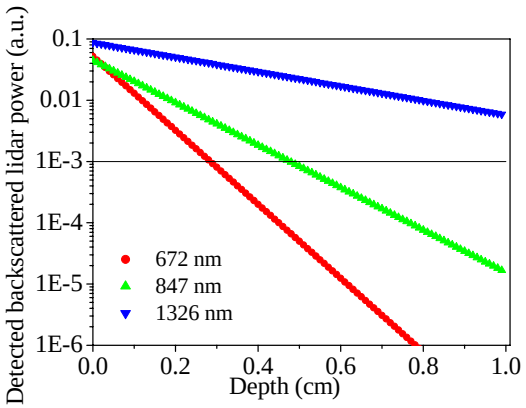

Figure 6. Dependence on depth of the return-signal power at single-sided lidar-type diagnostics of Intralipid dilution of 0.2% concentration for different radiation wavelengths.

The results represented in figure 6 are calculated by using (2)-(5). It is evident that the longer wavelength would ensure deeper informative sensing and diagnostics. From another point of view, however, the longer-wavelength radiations within the therapeutic window undergo stronger absorption in water, which may lead to undesirable increase of the temperature of the diagnosed in vivo tissues. When a laser beam/pulse of effective duration τ_p is propagating through a watery turbid medium, in the small-angle-approximation zone [16], the heat deposition and the temperature rise T along the beam axis can be estimated, using the expression (see also in [9,24])

$$T(z) = \mu_a P_t \tau_p [\pi w^2(z)\rho c_t]^{-1} \exp(-\mu_a z) , \quad (6)$$

where P_t is the peak pulse power, $w(z)$ is the beam radius at depth z, and ρ and c_t are, respectively, the mass density and the specific thermal capacity of water. When z decreases, $w(z)$ tends to the initial beam radius w. On the contrary, when z increases and approaches the developed scattering zone, $w^2(z) = \mu_{rs} z^3/6 >> w$ [16]. So, it is clear [see (6)] that the temperature increment T is maximum at the entrance into the medium, when $z \to 0$. Then we have

$$T(z=0) = \mu_a P_t \tau_p [\pi w^2 \rho c_t]^{-1} . \quad (7)$$

Assume further, taking into account the recommendations of the American National Standards Institute and the International Electrotechnical Commission about the safe, maximum permissible exposures to laser radiation [25], that $\lambda = 1326$ nm, $\mu_a = 2.16$ cm^{-1} [12], the pulse energy $E_p = P_t \tau_p = 8\mu J$, $P_t = 38$ mW, $w = 1$ mm, $\rho = 1000$ kg/m^3, and $c_t = 4186$ Jkg^{-1}K^{-1}. Under such conditions, we obtain that $T(0) \sim 1.314\text{x}10^{-4}$ K per a pulse. The thermal relaxation time τ_r of the heated region (of length μ_a^{-1} and radius w) is [9,26]

$$\tau_r \sim \min [(4\mu_a)^{-2}, (w/2)^2]/k_d , \quad (8)$$

where $k_d = k_c /(\rho c_t)$ is thermal diffusivity, and k_c is thermoconductivity. For water, $k_c \cong 0.58$ W/(mK) and respectively $k_d \cong 1.38 \times 10^{-7}$ m^2/s. Then, using (8) we obtain that $\tau_r \sim 2$ s. The lidar type sensing of tissues would require many laser shots along one line of sight in order to accumulate a sufficient statistical volume for accurate signal estimation [23]. The pulse repetition rate of sensing however will be restricted by the thermal relaxation time τ_r. So, if we do not like that T exceeds ~ 0.5 K during the sensing procedure, the pulse repetition rate should not exceed 2000 Hz, that is 4000 laser shots and 32 mJ deposited light energy during every 2 s long time interval. Then, the maximum temperature rise, near the entrance of the laser beam into the investigated medium, will be 0.523 K. If one should deposit, for instance, 3.2 J radiative energy in order to achieve a prescribed signal-measurement accuracy to a given depth, the sensing procedure should evidently last 200 s.

In general, a careful selection is necessary of optimum sensing conditions ensuring optimum diagnostic safety and convenience, accuracy and resolution, and, respectively, depth of reliable detection of characteristic more or less contrasting inhomogeneities.

5. Conclusion

In this work, we have investigated experimentally the extinction coefficient of IL-20% dilutions in distilled water, depending on the IL concentration, for several laser radiation wavelengths in the red and near-infrared regions. The approach to measuring the extinction coefficient has been developed by us recently. It is based on the specific behavior in the low-scattering zone of the on-axis intensity of laser radiation beams propagating through the investigated media. The measurements have been conducted, using separately two dilution-containing plexiglass boxes of different volumes, in order to prove the appropriateness of the assumption of semi-infinite turbid medium.

The experimental results for the extinction are in agreement with our previous results concerning the dependence of μ_e on C. They are also in agreement with empiric formulae found by other authors [6-8] concerning the wavelength dependence of μ_s of IL-10% and IL-20% dilutions. It has been shown as well that the values obtained for the extinction coefficient do not depend on the choice of the plexiglass container and tend to the water absorptance at vanishing IL concentration.

As a whole, the results obtained in the work confirm the consideration of the experimental phantoms as semi-infinite media. They also confirm and extend theoretical and experimental results obtained previously, and reveal advantages of using relatively long wavelengths (around the upper limit of the therapeutic window) for deeper sensing and diagnostics of tissues and mimicking turbid media.

Acknowledgments

This work has been supported in part by the Bulgarian National Science Fund under the project "Development of biophotonics methods as a basis of oncology theranostics".

References

[1] Gibson A P, Hebden, J C and Arridge S R 2005 *Phys. Med. Biol.* **50** R1–R43
[2] Drexler W and Fujimoto J G 2008 Optical *Coherence Tomography: Technology and Applications* (Berlin: Springer)
[3] Taroni P et al. 2010 *J. Biomed. Opt.* **15** 060501
[4] Flock S T, Jacques S L, Wilson B C, Star W M and van Gemert M J C 1992 *Lasers Surg. Med.* **2** 510–9
[5] Ninni P D, Martelli F and Zaccanti G 2011 *Phys. Med. Biol.* **56** N21
[6] van Staveren H J, Moes, C J M, van Marie J, Prahl S A and van Gemert M J C 1991 *Appl. Opt.* **30** 4507-14
[7] Michels R, Foschum F and Kienle A 2008 *Opt. Express* **16** 5907-25
[8] Aernouts B, Zamora-Rojas E, Van Beers R, Watté R, Wang L, Tsuta M, Lammertyn J and Saeys W 2013 *Opt. Express* **21** 32450
[9] Kim A and Wilson B C 2011 Measurement of *ex vivo* and *in vivo* tissue optical properties:

methods and theories *Optical-Thermal Response of Laser-Irradiated Tissue* 2nd edn ed A J Welch and M J C van Gemert (Berlin: Springer) chapter 8, p.267
[10] Jacques S L 2013 *Phys. Med. Biol.* **58** R37–R61
[11] Palmer K F and Williams D 1974 *JOSA* **64** 1107-10
[12] Wieliczka D M, Weng S and Querry M R 1989 *Appl. Opt.* **28** 1714-19
[13] Pope R M and Fry E S 1997 *Appl. Opt.* **36** 8710-23
[14] Anderson R R and Parrish J A 1981 *J. Invest. Dermatol.* **77** 13–19
[15] Gurdev L, Dreischuh T, Bliznakova I, Vankov O, Avramov L and Stoyanov D 2012 *Phys. Scripta* **T149** 014074
[16] Gurdev L. Dreischuh T, Vankov O, Bliznakova I, Avramov L and Stoyanov D 2014 *Appl. Phys. B* **11**5 427-41
[17] Ishimaru A 1978 *Wave Propagation and Scattering in Random Media* Vol. 1 (New York: Academic Press)
[18] Campbell S D, Menon S, Rutherford G, Su Q and Grobe R 2007 *Laser Physics* **17** 117-23
[19] Marchesini R, Bertoni A, Andreola S, Melloni E and Sichirollo A 1989 *Appl. Opt.* **28** 2318-24
[20] Zaccanti G, Bianco, S and Martelli, F 2003 *Appl. Opt.* **42** 4023–30
[21] Giusto A, Saija R, Iatì M A, Denti P, Borghese F and Sindoni O I 2003 *Appl. Opt.* **42** 4375-80
[22] Gurdev L, Dreischuh T and Stoyanov D 2011 Deconvolution of long-pulse lidar profiles *Lasers – Applications in Science and Industry* ed K Jakubczak (Vienna: Intech) chapter 13 pp 249-276
[23] Gurdev L, Dreischuh T and Stoyanov D 2007 *Proc. SPIE* **6604** 66042I
[24] Walsh J T 2011 Basic interactions of light with tissue *Optical-Thermal Response of Laser-Irradiated Tissue* 2nd edn ed A J Welch and M J C van Gemert (Berlin: Springer) chapter 2, p.13
[25] Gould T, Wang Q, Pfefer T J 2014 *Biomed. Opt. Express* **5** 832-847
[26] Cox, B 2013 *Introduction to Laser-Tissue Interactions* Lecture notes MPHY3886/M866/G886: Optics in Medicine (London: University College London, UK)